Charge and spin degrees of freedom in *A*-site ordered $YCu_3Co_4O_{12}$ and $CaCu_3Co_4O_{12}$

Yi-Ying Chin,[1,*] Zhiwei Hu,[2] Yuichi Shimakawa,[3] Junye Yang,[4] Youwen Long,[4,5] A. Tanaka,[6] Liu Hao Tjeng,[2] Hong-Ji Lin,[7,†] and Chien-Te Chen[7]

[1]*Department of Physics, National Chung Cheng University, Chiayi 62102, Taiwan*
[2]*Max Planck Institute for Chemical Physics of Solids, Nöthnitzer Strasse 40, 01187 Dresden, Germany*
[3]*Institute for Chemical Research, Kyoto University, Kyoto 611-0011, Japan*
[4]*Beijing National Laboratory for Condensed Matter Physics, Institute of Physics, Chinese Academy of Sciences, Beijing 100190, China*
[5]*Songshan Lake Materials Laboratory, Dongguan, Guangdong 523808, China*
[6]*Quantum Matter Program, Graduate School of Advanced Science and Engineering, Hiroshima University, Higashi-hiroshima 739-8530, Japan*
[7]*National Synchrotron Radiation Research Center (NSRRC), 101 Hsin-Ann Road, Hsinchu 30076, Taiwan*

(Received 28 December 2020; accepted 11 March 2021; published 26 March 2021)

Using soft x-ray absorption spectroscopy we were able to determine unambiguously the charge and spin states of the transition metal ions in stoichiometric $YCu_3Co_4O_{12}$ and $CaCu_3Co_4O_{12}$. The trivalent and low-spin nature of both the Cu and Co ions in $YCu_3Co_4O_{12}$ makes this correlated system to be effectively a nonmagnetic band semiconductor. The substitution of Y by Ca produces formally tetravalent Co ions but the doped holes are primarily on the oxygen ligands. Concerning the spin degrees of freedom, the trivalent Co ions in $YCu_3Co_4O_{12}$ remain low spin upon the Y-Ca substitution, very much unlike the $La_{1-x}Sr_xCoO_3$ system. The tetravalent Co ions in $CaCu_3Co_4O_{12}$ are interestingly also in the low-spin state, which then explains the good electrical conductivity of $CaCu_3Co_4O_{12}$ since charge exchange between neighboring Co^{3+} and Co^{4+} ions will not be hampered by the spin-blockade mechanism that otherwise would be in effect if the Co^{4+} and Co^{3+} spin quantum numbers were to differ by more than one-half. We infer that the stability of the Co low-spin state is related to the very short Co-O bond lengths.

DOI: 10.1103/PhysRevB.103.115149

I. INTRODUCTION

The oxides $YCu_3Co_4O_{12}$ and $CaCu_3Co_4O_{12}$ belong to material class of the *A*-site ordered perovskites $AA'_3B_4O_{12}$ [1]. The A′ = Cu ions are coordinated by four oxygens in a square planar symmetry and the *B* = Co ions form CoO_6 octahedra in a cubic ABO_3 perovskite structure. Figure 1 displays the crystal structure. $YCu_3Co_4O_{12}$ and $CaCu_3Co_4O_{12}$ are unique in the sense that they contain transition metal ions in a very high oxidation state, i.e., the Co ions need to be tetravalent or the Cu ions trivalent. These are chemically high energy configurations, requiring the material be synthesized under high pressures followed by rapid cooling and slow pressure release at low temperatures [1]. The question whether the Co ions are actually tetravalent or trivalent, and correspondingly, the Cu ions are divalent or trivalent, was the starting point of a band structure study [2]. There is a strong competition between having the Co^{4+} configuration stabilized in the material or instead the Cu^{3+}. Electrical transport studies reveal that $YCu_3Co_4O_{12}$ is an insulator while $CaCu_3Co_4O_{12}$ shows a metallic behavior [1]. This, together with a bond-valence-sum analysis of the powder diffraction data, suggests that the $YCu_3{}^{3+}Co_4{}^{3+}O_{12}$ and $CaCu_3{}^{3+}Co_4{}^{3.25+}O_{12}$ scenarios are in place [1]. The band structure study [2] as well as an x-ray photoelectron spectroscopy investigation [3] supported these charge scenarios. The Jahn-Teller effect associated with the square planar coordination of the Cu ions and their trivalent state led to further studies [4–8] that also pointed out the importance of Zhang-Rice physics in this material class.

Another intriguing aspect of $YCu_3Co_4O_{12}$ and $CaCu_3Co_4O_{12}$ concerns the spin state of the Co ions. It is well known that a Co^{3+} ion can be in a low-spin (LS) or high-spin (HS) state depending on the details of the Co local coordination [9–12]. Even the intermediate-spin (IS) situation is a possibility, although it would require an extraordinarily distorted coordination [13–15]. Similarly, a Co^{4+} ion can be found in a LS, IS, and perhaps also HS state depending on the local Co coordination [16–20]. The schematic one-electron energy level diagram for Co^{3+} as well as Co^{4+} is displayed in Fig. 2. The situation for $YCu_3Co_4O_{12}$ and $CaCu_3Co_4O_{12}$ is not clear. Several studies favor the LS state for both the Co^{3+} and Co^{4+} ions [2–4], while others predict the IS state to emerge upon Y-Ca substitution [5,7,8]. In this respect it is worth noting that hole-doping of $LaCoO_3$ by La-Sr/Ca substitution leads to the formation of spin-state polarons in which the Co^{3+} ions surrounding each Sr/Ca convert their spin state from LS to IS or HS [21–25].

Here we address the spin state of the Co ions in $YCu_3Co_4O_{12}$ and $CaCu_3Co_4O_{12}$ using an experimental method that is element specific and extremely sensitive to the charge and spin states of the transition metal (TM) ions, namely soft x-ray absorption spectroscopy (XAS) at the

*Corresponding author: yiyingchin@ccu.edu.tw
†hjlin@nsrrc.org.tw

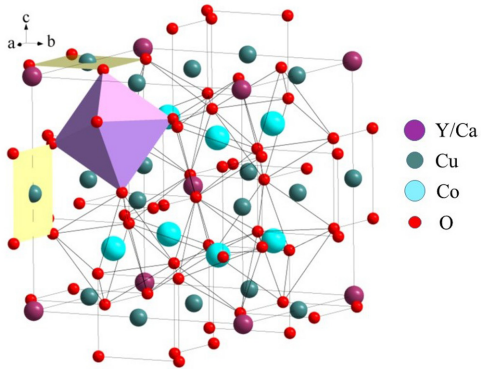

FIG. 1. Crystal structure of $YCu_3Co_4O_{12}$ and $CaCu_3Co_4O_{12}$. The Cu ions are coordinated by four oxygens in a square planar symmetry and the Co ions form CoO_6 octahedra in a cubic ABO_3 perovskite structure.

TM-$L_{2,3}$ and O-K edges [9–15,17–20]. We will investigate the spin states of the Co^{3+} and Co^{4+} ions, and we will study whether or not there is a spin-state transition upon Y-Ca substitution. Our objective is to explain why the Y compound behaves effectively like a nonmagnetic semiconductor and why the Ca variant shows such good electrical conductivity. Since high-oxidation state materials have often the tendency to be oxygen deficient, we also will need to verify the stoichiometry of the samples by measuring also the oxidation states of the Cu and Co ions in our spectroscopic experiment.

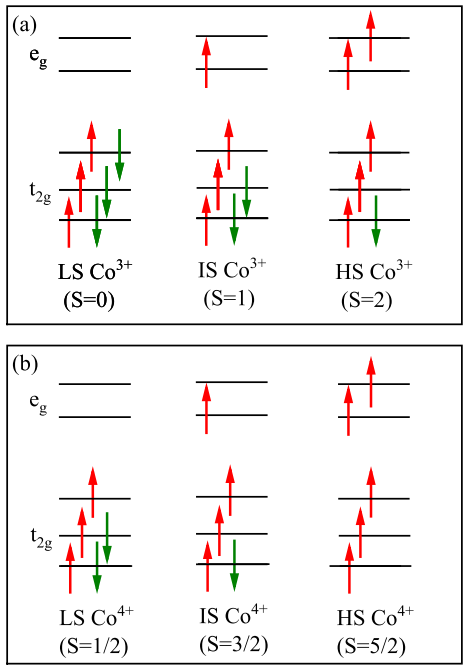

FIG. 2. Schematic one-electron energy level diagram for a Co^{3+} $3d^6$ [top panel (a)] and a Co^{4+} $3d^5$ ion [bottom panel (b)] in octahedral symmetry. The e_g and t_{2g} orbital occupations and the total spin quantum number S are indicated for the low-spin (LS), intermediate-spin (IS), and high-spin (HS) configuration.

II. EXPERIMENT

The $CaCu_3Co_4O_{12}$ and $YCu_3Co_4O_{12}$ materials were prepared from stoichiometric mixtures as described elsewhere [1]. $SrCoO_3$ was also included in this study to serve as a Co^{4+} reference [26]. The soft x-ray absorption experiments at the O-K, Co-$L_{2,3}$, and Cu-$L_{2,3}$ edges have been performed at the BL11A beamline of the National Synchrotron Radiation Research Center (NSRRC) in Taiwan. The energy resolution at the O-K is set at about 0.15 eV, while it was 0.25 eV for the Co-$L_{2,3}$ and 0.3 eV for the Cu-$L_{2,3}$. The O-K and Cu-$L_{2,3}$ XAS data were obtained in the fluorescence yield (FY) mode, while the Co-$L_{2,3}$ XAS spectra were collected in the total electron yield (TEY) mode. The FY mode has the advantage of a larger probing depth but may suffer from self-absorption effects which could complicate the interpretation. Practice shows that FY works well for the O-K edge: self-absorption effects are small/negligible [27]. FY can also be used for the Cu-$L_{2,3}$ edges: if the spectrum consists of a single peak, then self-absorption corrections [27] can provide reliable results since it will not alter its energy position nor change the number of peaks as we show in the Appendix. For the Co-$L_{2,3}$ edges, however, we rely heavily on the line shape of the spectra and self-absorption corrections may change the fine details in the line shape. We have therefore utilized the TEY mode to ensure that the correct line shape is being recorded. The samples were cleaved in the ultrahigh vacuum chamber of the beamline with a base pressure in the 10^{-10} mbar range and the measurements have been carried out at room temperature. Single crystals of CoO, CuO, and NiO were measured simultaneously in a separate chamber to serve as energy references for the Co-$L_{2,3}$, Cu-$L_{2,3}$ and the O-K edges, respectively.

III. RESULTS

Figure 3 shows the Cu-L_3 XAS spectra of $CaCu_3Co_4O_{12}$ and $YCu_3Co_4O_{12}$ together with those of CuO as a Cu^{2+} reference and $NaCuO_2$ [28] as a Cu^{3+} reference. The energy position of the white line of A-site ordered perovskites is considerably higher than that of CuO [29], indicating that the Cu in $CaCu_3Co_4O_{12}$ and $YCu_3Co_4O_{12}$ is not divalent. On the other hand, the energy positions of the $CaCu_3Co_4O_{12}$, $YCu_3Co_4O_{12}$, and $NaCuO_2$ are very similar, revealing that the Cu in $CaCu_3Co_4O_{12}$ and $YCu_3Co_4O_{12}$ is trivalent. Indeed, it is known for open shell systems that an increase of the valence of the TM ion by one results in a shift of the $L_{2,3}$ XAS spectrum to the higher energies by about 1–2 eV with the energy difference given by that between the $2p$-$3d$ Coulomb interaction and the $3d$-$3d$ counterpart [17,30,31]. We would like to note that our $CaCu_3Co_4O_{12}$ and $YCu_3Co_4O_{12}$ spectra consist of a single peak and differ from those reported earlier in the literature [7,8] where a second additional impurity peak was present.

After determining the Cu valence, we now turn to the Co-$L_{2,3}$ XAS spectra to investigate the Co. The spectra of $YCu_3Co_4O_{12}$ and $CaCu_3Co_4O_{12}$ are presented in Fig. 4, together with those of CoO, $EuCoO_3$, and $SrCoO_3$. The latter three serve as reference for Co^{2+}, LS Co^{3+}, and Co^{4+}, respectively. The line shape of the $YCu_3Co_4O_{12}$ spectrum is similar to that of the LS Co^{3+} reference, but different from those of

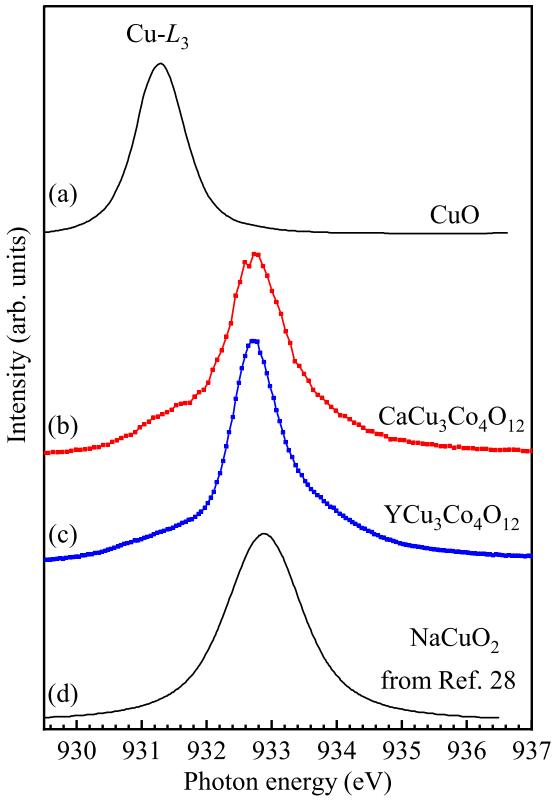

FIG. 3. Cu-L_3 XAS spectra of $CaCu_3Co_4O_{12}$ (b) and $YCu_3Co_4O_{12}$ (c) together with those of CuO as a Cu^{2+} reference (a) and $NaCuO_2$ as a Cu^{3+} reference (d). The $NaCuO_2$ spectrum is reproduced from Ref. [28].

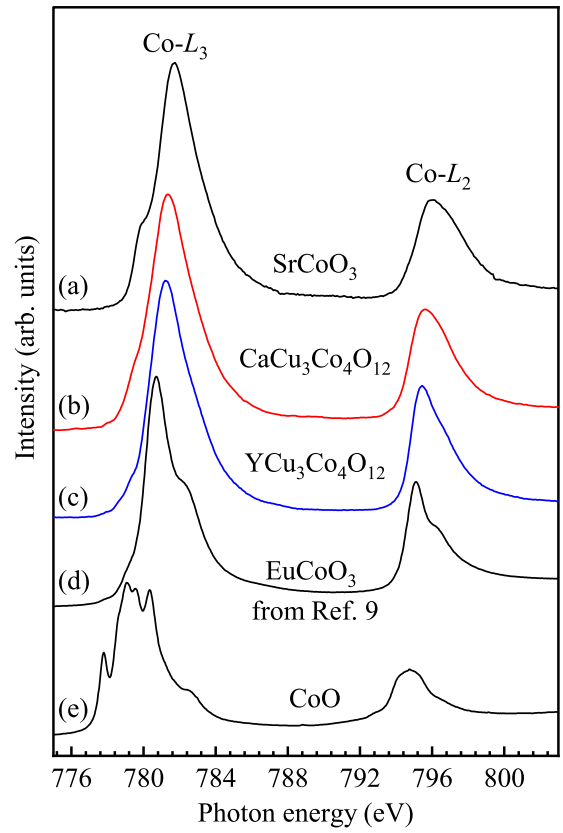

FIG. 4. Co-$L_{2,3}$ XAS spectra of $CaCu_3Co_4O_{12}$ (b) and $YCu_3Co_4O_{12}$ (c) together with those of CoO (e) as a Co^{2+} reference, $EuCoO_3$ (d) as a LS Co^{3+} reference (reproduced from Ref. [9]), and $SrCoO_3$ (a) as a Co^{4+} reference.

the Co^{2+} and Co^{4+} references. These results indicate that the Co is trivalent in $YCu_3Co_4O_{12}$, fulfilling the charge balance requirement imposed by the finding above that the Cu is trivalent. In turn, the results also confirm that the $YCu_3Co_4O_{12}$ sample has the correct oxygen stoichiometry.

We would like to remark that the $YCu_3Co_4O_{12}$ spectrum is somewhat broader than that of $EuCoO_3$. We attribute this to the presence of the Cu ions which (unlike Eu) can have appreciable hybridization with the Co [2,4,5,7]. In fact, the superexchange interactions between the Cu and the magnetic B,B' ions reported in $ACu_3B_2B'_2O_{12}$ (B = Fe, B' = Re,Os) [32,33] are based on the presence of such hybridization processes. Yet, the overall line shape including the L_2/L_3 branching ratio [34,35] in the Co-$L_{2,3}$ spectra of $YCu_3Co_4O_{12}$ and $EuCoO_3$ are quite similar, indicating not only the trivalent state for the Co in $YCu_3Co_4O_{12}$ but also the LS state. The aspect that all the Co^{3+} are in the LS state makes it more favorable for $YCu_3Co_4O_{12}$ to be a good insulator [1,3,4] since it is known from $LaCoO_3$ that it loses quickly its highly insulating nature as soon as the LS to IS or HS state transition takes place with temperature. Moreover, with all the Cu and Co ions being trivalent and low spin, we can readily envision that this correlated material is an insulator since we can map its electronic structure onto that of a band semiconductor having nonmagnetic ions and even number electrons per formula unit cell.

Figure 4 reveals that the spectrum of $CaCu_3Co_4O_{12}$ is not very different from that of $YCu_3Co_4O_{12}$ despite the fact that the charge count on the Co ions have been altered by one (per formula unit). This suggests that most of the Co ions have not changed their local electronic state, namely LS Co^{3+}. In order to unveil the effect of the hole doping, we need to look more carefully and carry out the following analysis. Assuming that on average ¾ of the Co ions keep their LS trivalent state in $CaCu_3Co_4O_{12}$, we can try to remove their contribution to the $CaCu_3Co_4O_{12}$ spectrum so that we are left with a spectrum that reflects solely the changes due to the hole doping. In order to do so, we can use the $YCu_3Co_4O_{12}$ spectrum scaled by a factor ¾ to represent the LS Co^{3+} ions in $CaCu_3Co_4O_{12}$. The results are presented in Fig. 5.

The top panel of Fig. 5 shows the spectrum of $CaCu_3Co_4O_{12}$, ¾ times $YCu_3Co_4O_{12}$ and their difference. The line shape of the difference spectrum is very different from that of $YCu_3Co_4O_{12}$ itself or $EuCoO_3$ (see also Fig. 4). The Co-L_3 white line of the difference spectrum is also at a higher energy position than that of the $YCu_3Co_4O_{12}$. This implies that the hole doping due to Ca-Y substitution indeed produces Co ions that are not LS Co^{3+} but rather Co^{4+}. We may speculate that these Co^{4+} ions could be localized primarily around the Ca ions: we may draw a parallel to the case of $LaCoO_3$ where La substitution by Sr or Ca produces spin-state polarons [21–25]. Our next task is to determine whether the

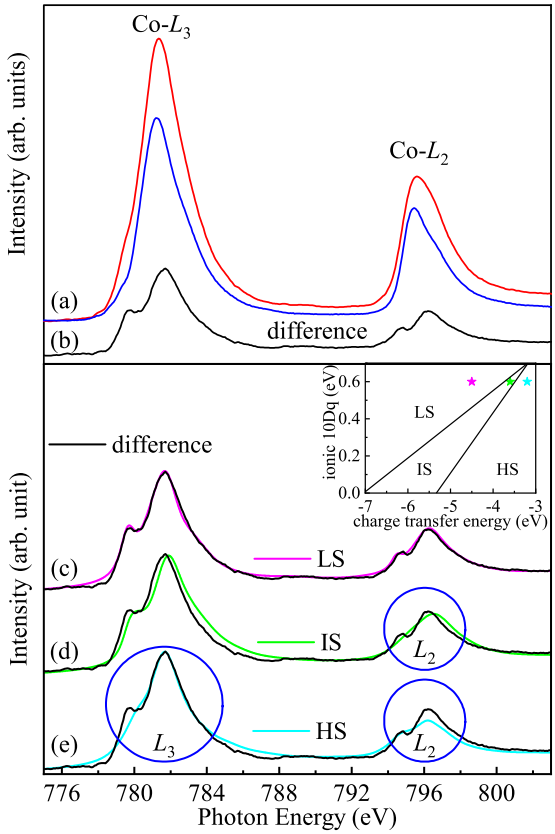

FIG. 5. Top panel: Co-$L_{2,3}$ XAS spectrum of $CaCu_3Co_4O_{12}$ (a, red curve), $YCu_3Co_4O_{12}$ scaled by a factor ¾ (a; blue curve), and their difference spectrum (b, black curve). Bottom panel: Enlarge view on the difference spectrum (c,d,e, black curve) together with the theoretical spectrum for a Co^{4+} LS (c, magenta), IS (d, green), and HS (e, cyan). The inset shows the parameters used in the Co^{4+} cluster calculations which generated the LS, IS, and HS theoretical spectra. Circles indicate regions of discrepancy between experiment and the calculated spectra.

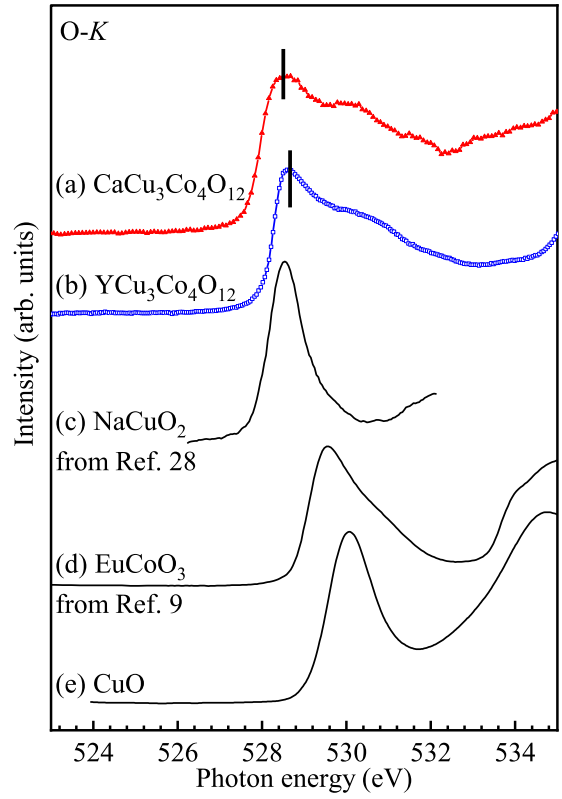

FIG. 6. O-K XAS spectra of $CaCu_3Co_4O_{12}$ (a), $YCu_3Co_4O_{12}$ (b), $NaCuO_2$ (c), $EuCoO_3$ (d), and CuO (e). The $NaCuO_2$ spectrum is reproduced from Ref. [28], and the $EuCoO_3$ spectrum from Ref. [9].

spectrum can be matched with that of a Co^{4+} in a LS, IS, or HS state.

We have simulated the Co-$L_{2,3}$ XAS spectrum using a CoO_6 cluster model which includes configuration interaction and full atomic multiplet theory, an approach that is very successful to quantitatively explain the line shape in many XAS spectra of 3d TM oxides [36,37]. The XTLS 9.0 code [36] has been used. Here we have calculated the spectra for a $Co^{4+}O_6$ cluster with the $3d^5$ LS, IS, and HS state configurations. The parameters are listed in Ref. [38]. The results are displayed in the bottom panel of Fig. 5. We can clearly observe that the LS scenario gives the best match to the experimental difference spectrum. The IS simulation, on the other hand, reveals discrepancies in the L_2 region as marked by a blue circle. The HS case has even larger deviations, not only in the L_2 but also in the L_3 regions, see the respective blue circles in the bottom panel of Fig. 5.

The good simulation that we have been able to achieve for the difference spectrum, i.e., LS Co^{4+}, also justifies retrospectively the assumption that on average ¾ of the Co ions remain in their LS trivalent state in $CaCu_3Co_4O_{12}$. We therefore can conclude that the charge configuration of our A-site ordered perovskites are $YCu_3{}^{3+}Co_4{}^{3+}O_{12}$ and $CaCu_3{}^{3+}Co_4{}^{3.25+}O_{12}$, and that both the Co^{3+} and Co^{4+} ions are in the LS state. We can definitely rule out spectroscopically a $CaCu_3{}^{2+}Co_4{}^{4+}O_{12}$ or a $YCu_3{}^{2+}Co_4{}^{3.75+}O_{12}$ scenario, since this would have implied that $CaCu_3Co_4O_{12}$ would have magnetic ions and could become a Mott insulator, while $YCu_3Co_4O_{12}$ would then be a metallic doped Mott material, respectively. On the contrary, reality tells us indeed that $CaCu_3Co_4O_{12}$ is metallic and $YCu_3Co_4O_{12}$ insulating [1,3], consistent with our spectroscopic findings.

In the $Co^{4+}O_6$ cluster calculations we have used the $3d^5$, $3d^6\underline{L}$, $3d^7\underline{L}^2$, and $3d^8\underline{L}^3$ configuration, whereby $\underline{L}$ denotes a hole in the O 2p ligand. In order to get a good match between experiment and simulation, we need to use negative values for the O 2p to Co 3d charge transfer energy. The values are indicated in the inset of Fig. 5. Negative charge transfer energies mean that the $3d^5$ is not the lowest in energy but rather the $3d^6\underline{L}$. This in turn implies that the doped hole (as a result of the Y-Ca substitution) resides more on the O 2p ligand states rather than on the Co 3d.

Figure 6 presents the O-K XAS spectra of $CaCu_3Co_4O_{12}$ and $YCu_3Co_4O_{12}$ together with those of $NaCuO_2$ [28], $EuCoO_3$ [9], and CuO. We observe that the CuO has its O-K white line at 530.1 eV, the $EuCoO_3$ at 529.6 eV, and the $NaCuO_2$ at an appreciable lower energy of 528.5 eV. CuO serves here as a Cu^{2+} compound, $EuCoO_3$ as an LS Co^{3+},

and $NaCuO_2$ as a Cu^{3+}. The white line of $YCu_3Co_4O_{12}$ is at the low value of 528.6 eV. As we have shown from the Cu and Co $L_{2,3}$ XAS measurements above, $YCu_3Co_4O_{12}$ contains Cu^{3+} and LS Co^{3+} ions. The white line of $YCu_3Co_4O_{12}$ can therefore be attributed to the $1s \rightarrow 2p$ transitions on the O ions which surround the Cu^{3+} ions. The white line of $CaCu_3Co_4O_{12}$ is at 528.5 eV, slightly lower than that of the Y compound. As shown above, $CaCu_3Co_4O_{12}$ contains Cu^{3+}, LS Co^{3+}, and LS Co^{4+} species. We thus may attribute its white line now to not only the O ions surrounding the Cu^{3+} but also to the O surrounding the Co^{4+} ions. Our reason for involving the Co^{4+} here is given by the observation that the spectrum of $CaCu_3Co_4O_{12}$ shows a broadening to the low energy side of its white line in comparison to that of $YCu_3Co_4O_{12}$, indicating that the Y-Ca substitution introduces an additional state at the lowest energy. In the following we would like to explain why Cu^{3+} and Co^{4+} produce states in the O-K XAS with very low energies.

A minimal model to interpret O-K XAS spectra for TM oxides requires the consideration of two configurations for the ground state problem, namely $d^n p^6$ and $d^{n+1}p^5$, where d denotes the TM $3d$ shell and p the O $2p$. Here n denotes the number of electrons in the TM $3d$ shell, which is $n = 9$ for Cu^{2+}, $n = 8$ for Cu^{3+}, $n = 6$ for Co^{3+}, and $n = 5$ for Co^{4+}. The O-K transition is possible when there is a hole in the O $2p$ shell and can be described by the equation $p^5 + h\nu(\mathrm{O}) \rightarrow \underline{c}p^6$, where $\underline{c}$ denotes the $1s$ core hole at the O site and $h\nu(\mathrm{O})$ the energy cost. This minimal model has thus one configuration for the final state problem, namely $d^{n+1}\underline{c}p^6$.

For Cu^{2+} and Co^{3+} compounds, the lowest energy configuration is given by $d^n p^6$ [10,29,39]. This configuration does not contribute to the O-K XAS since with p^6 there is no hole in the O $2p$ shell. However, the $d^n p^6$ configuration hybridizes with higher lying $d^{n+1}p^5$, thereby forming a ground state that has some hole in the O $2p$ shell. The O-K XAS is now possible and it basically probes the unoccupied O $2p$ states that are mixed with the unoccupied TM $3d$ states thereby revealing the multiplet structure of the d^{n+1} configuration of the TM [40]. The energy of the white line is then given by $h\nu(\mathrm{O}) + \Delta + \delta$, whereby the charge transfer energy Δ denotes the energy separation between $d^n p^6$ and $d^{n+1}p^5$ configurations [39] and δ the energy gain of the ground state due to $d^n p^6$ and $d^{n+1}p^5$ hybridization.

For Cu^{3+} and Co^{4+} compounds the lowest energy configuration is not $d^n p^6$ but $d^{n+1}p^5$. This is indicated in the model calculations for $NaCuO_2$ [41,42] by a negative value for Δ, similarly also for $SrCoO_3$ [16], Na_xCoO_2 [17], $BaCoO_3$ [20], and now for $CaCu_3Co_4O_{12}$ (inset in Fig. 5 and parameter list given in Ref. [38]). Having already holes in the $d^{n+1}p^5$, the O-K XAS can start from this lowest lying configuration. The energy of the white line is then given by $h\nu(\mathrm{O}) + \delta'$, whereby δ' denotes the energy gain of the ground state due to $d^{n+1}p^5$ and $d^n p^6$ hybridization. In other words, the (negative) Δ term is in the zeroth order not present so that the white lines of negative charge energy systems (Cu^{3+}, Co^{4+}) is lower by about $\Delta + \delta - \delta'$ in comparison to the white lines of positive charge transfer energy systems (Cu^{2+}, Co^{3+}). Here Δ denotes the charge transfer energy of the positive charge transfer energy system. We would like to note that δ and δ' need not be small quantities and that δ' is generally larger than δ since the hybridization is usually stronger for negative charge transfer systems. The result is then that the lowering of the O-K XAS peak position (when comparing negative with positive charge transfer systems) can be considerably less than Δ.

IV. DISCUSSION

We have found out from our experiments that upon hole doping via Ca-Y substitution most of the Co^{3+} ions do not change their local electronic state, i.e., they remain in the LS state. This is very different from the $La_{1-x}Sr_xCoO_3$ system, where hole doping by La-Sr/Ca substitution produces spin-state polarons in which the Co^{3+} ions in the vicinity of a Sr/Ca alter their spin state from LS to IS or HS [21–25]. We notice that the average Co-O bond length in $LaCoO_3$ is 1.925 Å at 5 K and 1.928 Å at 100 K [43]. At 5 K $LaCoO_3$ is completely nonmagnetic indicating that the Co^{3+} ions are all in the LS state. At 100 K, on the other hand, the magnetic susceptibility reaches a high nonzero value [43], implying that magnetic Co^{3+} ions are present. These observations seem to suggest that the LS to HS transition [10] takes place at a crossover distance of about 1.928 Å [12]: the LS (HS) is stable for short (long) distances since the effective crystal field is large (small). The spin state of $LaCoO_3$ may therefore be extremely sensitive to small changes in the local Co-O coordination induced by, for example, substitution of La by Sr/Ca. By contrast, the average Co-O distance in $YCu_3Co_4O_{12}$ and $CaCu_3Co_4O_{12}$ at 300 K is 1.9008 and 1.9037 Å, respectively [44]. These values are substantially smaller than 1.928 Å, explaining the high stability of the Co^{3+} LS state upon Y-Ca substitution.

Our experiment also revealed that in $CaCu_3Co_4O_{12}$ the Co^{4+} ion is in the LS state. We may be able to explain this finding by looking at the Co-O distances and comparing them to those in $Na_{0.75}CoO_2$, a material which is known to also have LS Co^{4+} ions [17]. As mentioned above, the average Co-O distance in $CaCu_3Co_4O_{12}$ is 1.9037 Å. For $Na_{0.75}CoO_2$, Co-O distances in the range 1.908–1.914 have been reported [45]. So the Co-O distances in $CaCu_3Co_4O_{12}$ are extremely short and this apparently ensures sufficiently large effective octahedral crystal field energies to stabilize the LS state for a $3d^5$ ion.

The finding that both the Co^{3+} and Co^{4+} ions in $CaCu_3Co_4O_{12}$ are in the LS state is in fact also an important aspect that one needs to take into account for explaining the metallic behavior of the compound. One can expect that in a mixed-valent situation an intersite exchange of charge between two sites P and Q of the type $Co^{3+}(\mathrm{P})Co^{4+}(\mathrm{Q}) \leftrightarrow Co^{4+}(\mathrm{P})Co^{3+}(\mathrm{Q})$ will not involve the high-energy on-site Coulomb interaction (Hubbard U). Still, the energy cost need not be zero. It depends very much on the spin states of the two sites. The system can be metallic if the total energy of the two sites before and after the charge exchange is equal, otherwise it will be semiconducting.

Figure 7(a) displays the LS Co^{3+} ($S = 0$) and LS Co^{4+} ($S = 1/2$) situation that we have found for $CaCu_3Co_4O_{12}$. Upon transferring an electron from the Co^{3+} to the Co^{4+} site we end up in a situation in which the Co^{3+} is converted into a LS Co^{4+} ($S = 1/2$) and the Co^{4+} into a LS Co^{3+}

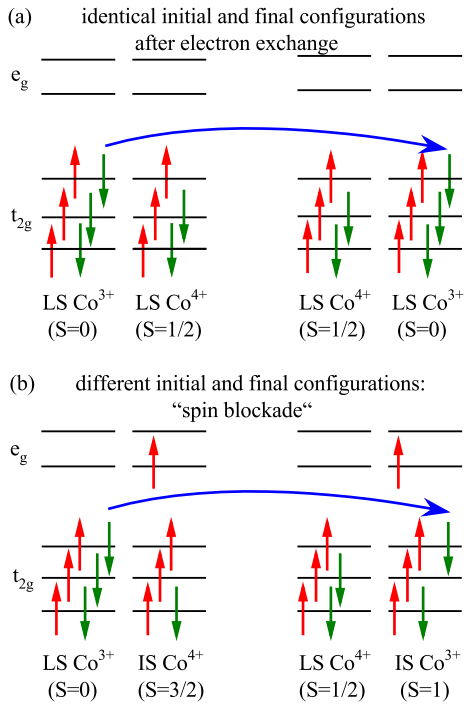

FIG. 7. Schematic diagram for an inter-site charge exchange between two neighboring Co sites in a mixed valent compound. Top panel: both the Co^{3+} ($S = 0$) and Co^{4+} ($S = 1/2$) sites are in the LS (low-spin) state; after the exchange of one electron, both Co ions are still in the LS state. Bottom panel: the Co^{3+} is LS ($S = 0$) and the Co^{4} IS (intermediate-spin, $S = 3/2$); after the electron exchange, the Co^{4+} is LS ($S = 1/2$) and the Co^{3+} IS ($S = 1$).

($S = 0$). Before and after the electron transfer we have in total the same spin state configuration, namely $S = 0$ and $S = 1/2$. The total energy before and after is identical, so the energy cost for the electron transfer is thus zero. Figure 7(b) illustrates an alternative scenario in which the Co^{4+} in the IS state ($S = 3/2$) while the Co^{3+} is LS ($S = 0$). A transfer of an electron from Co^{3+} to Co^{4+} will then end in a situation with a LS Co^{4+} ($S = 1/2$) and an IS Co^{3+} ($S = 1$). The spin-state situation before and after the electron exchange is thus quite different. Consequently, the total energies will be different and the electron transfer thus involves a nonzero energy cost. This mechanism is known as "spin-blockade" and has been invoked in order to explain the semiconducting behavior of $HoBaCo_2O_{5.5}$ [46] and $La_{1.5}Sr_{0.5}CoO_4$ [47].

V. SUMMARY

The Cu-L_3 XAS spectra of our stoichiometric $YCu_3Co_4O_{12}$ and $CaCu_3Co_4O_{12}$ material confirmed that the valence state of the Cu ions in both systems are 3+. The Co-$L_{2,3}$ XAS spectrum for $YCu_3Co_4O_{12}$ also revealed that the Co ions are all low spin 3+. With an even number of electrons per formula unit, and with all the Cu and Co ions in a nonmagnetic state, we infer that the insulating behavior of this correlated $YCu_3Co_4O_{12}$ system can be modeled in terms of an effective band semiconductor. Upon Ca substitution for Y, our Co-$L_{2,3}$ XAS spectrum indicated that the hole doping produced low spin Co^{4+} ions. Remarkably, the remaining Co^{3+} ions persisted in their low-spin state. We attribute the stability of the low spin nature of the Co^{4+} and Co^{3+} ions in $CaCu_3Co_4O_{12}$ to the very short Co-O distances. The presence of low spin Co^{4+} next to low spin Co^{3+} allowed us to explain the metallic behavior of $CaCu_3Co_4O_{12}$ in terms of charge transport in a mixed valent system that is not hindered by a spin-blockade mechanism, which otherwise would have occurred if the spin difference between the Co^{4+} and Co^{3+} ions were larger than one-half.

ACKNOWLEDGMENTS

This work was supported by the Ministry of Science and Technology of the Republic of China (MOST Grants No. 106-2112-M-213-003-MY3, No. 107-2112-M-194-001-MY3, and No. 109-2112-M-194-004-MY3), the National Key R&D Program of China (Grants No. 2018YFE0103200 and No. 2018YFA0305700), and the National Natural Science Foundation of China (Grants No. 11934017, No. 51772324, and No. 11921004). We also acknowledge the support from the Max Planck-POSTECH-Hsinchu Center for Complex Phase Materials. This work was partly supported by JSPS Grants-in-Aid for Scientific Research (19H05823 and 20H00397) and Core-to-Core Program (A) Advanced Research Networks in Japan.

APPENDIX: SELF-ABSORPTION CORRECTION

The Cu-L_3 XAS spectra of $CaCu_3Co_4O_{12}$ and $YCu_3Co_4O_{12}$ were taken in the fluorescence yield (FY) mode. They are displayed as black curves in Fig. 8. A correction for the self-absorption effects was applied following the recipe described in Ref. [27]. The results are plotted as red curves in Fig. 8.

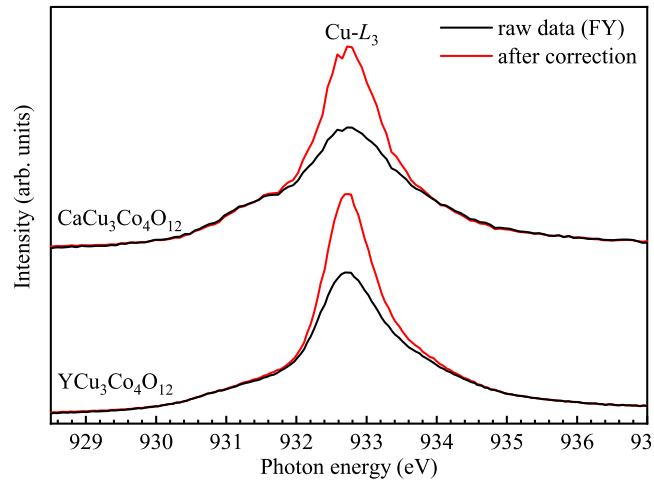

FIG. 8. Cu-L_3 XAS spectra of $CaCu_3Co_4O_{12}$ and $YCu_3Co_4O_{12}$. Black curves are the raw data taken in the fluorescence yield (FY) mode and red curves are the spectra after correction [27] for the self-absorption effects in the FY.

[1] I. Yamada, S. Ishiwata, I. Terasaki, M. Azuma, Y. Shimakawa, and M. Takano, Synthesis, structure, and physical properties of a-site ordered perovskites $ACu_3Co_4O_{12}$ (A = Ca and Y), Chem. Mater. **22**, 5328 (2010).

[2] H. P. Xiang, X. J. Liu, J. Meng, and Z. J. Wu, Structural stability and magnetic coupling in $CaCu_3Co_4O_{12}$ from first principles, J. Phys.: Condens. Matter **21**, 045501 (2009).

[3] T. Mizokawa, Y. Morita, T. Sudayama, K. Takubo, I. Yamada, M. Azuma, M. Takano, and Y. Shimakawa, Metallic versus insulating behavior in the A-site ordered perovskite oxides $ACu_3Co_4O_{12}$ (A = Ca and Y) controlled by Mott and Zhang-Rice physics, Phys. Rev. B **80**, 125105 (2009).

[4] P. Alippi and V. Fiorentini, Magnetism and unusual Cu valency in quadruple perovskites, Eur. Phys. J. B **85**, 82 (2012).

[5] S. Mukherjee, S. Sarkar, and T. Saha-Dasgupta, First-principles study of $CaCu_3B_4O_{12}$ (B = Co, Rh, Ir), J. Mater. Sci. **47**, 7660 (2012).

[6] T. Mizokawa, Jahn-Teller effects in transition-metal compounds with small charge-transfer energy, J. Phys. Conf. Ser. **428**, 012020 (2013).

[7] D. Meyers, S. Mukherjee, J. G. Cheng, S. Middey, J. S. Zhou, J. B. Goodenough, B. A. Gray, J. W. Freeland, T. Saha-Dasgupta, and J. Chakhalian, Zhang-Rice physics and anomalous copper states in A-site ordered perovskites, Sci. Rep. **3**, 1834 (2013).

[8] D. Meyers, S. Middey, J. G. Cheng, S. Mukherjee, B. A. Gray, Y. Cao, J. S. Zhou, J. B. Goodenough, Y. Choi, D. Haskel, J. W. Freeland, T. Saha-Dasgupta, and J. Chakhalian, Competition between heavy fermion and Kondo interaction in isoelectronic A-site-ordered perovskites, Nat. Commun. **5**, 5818 (2014).

[9] Z. Hu, H. Wu, M. W. Haverkort, H. H. Hsieh, H. J. Lin, T. Lorenz, J. Baier, A. Reichl, I. Bonn, C. Felser, A. Tanaka, C. T. Chen, and L. H. Tjeng, Different Look at the Spin State of Co^{3+} Ions in a CoO_5 Pyramidal Coordination, Phys. Rev. Lett. **92**, 207402 (2004).

[10] M. W. Haverkort, Z. Hu, J. C. Cezar, T. Burnus, H. Hartmann, M. Reuther, C. Zobel, T. Lorenz, A. Tanaka, N. B. Brookes, H. H. Hsieh, H. J. Lin, C. T. Chen, and L. H. Tjeng, Spin State Transition in $LaCoO_3$ Studied Using Soft x-ray Absorption Spectroscopy and Magnetic Circular Dichroism, Phys. Rev. Lett. **97**, 176405 (2006).

[11] Z. Hu, H. Wu, T. C. Koethe, S. N. Barilo, S. V. Shiryaev, G. L. Bychkov, C. Schüßler-Langeheine, T. Lorenz, A. Tanaka, H. H. Hsieh, H.-J. Lin, C. T. Chen, N. B. Brookes, S. Agrestini, Y.-Y. Chin, M. Rotter, and L. H. Tjeng, Spin-state order/disorder and metal-insulator transition in $GdBaCo_2O_{5.5}$: Experimental determination of the underlying electronic structure, New J. Phys. **14**, 123025 (2012).

[12] J. M. Chen, Y. Y. Chin, M. Valldor, Z. Hu, J. M. Lee, S. C. Haw, N. Hiraoka, H. Ishii, C. W. Pao, K. D. Tsuei, J. F. Lee, H. J. Lin, L. Y. Jang, A. Tanaka, C. T. Chen, and L. H. Tjeng, A complete high-to-low spin state transition of trivalent cobalt ion in octahedral symmetry in $SrCo_{0.5}Ru_{0.5}O_{3-\delta}$, J. Am. Chem. Soc. **136**, 1514 (2014).

[13] S. Ya. Istomin, O. A. Tyablikov, S. M. Kazakov, E. V. Antipov, A. I. Kurbakov, A. A. Tsirlin, N. Hollmann, Y. Y. Chin, H.-J. Lin, C. T. Chen, A. Tanaka, L. H. Tjeng, and Z. Hu, An unusual high-spin ground state of Co^{3+} in octahedral coordination in brownmillerite-type cobalt oxide, Dalton Trans. **44**, 10708 (2015).

[14] Y. Y. Chin, H. J. Lin, Z. Hu, C. Y. Kuo, D. Mikhailova, J. M. Lee, S. C. Haw, S. A. Chen, W. Schnelle, H. Ishii, N. Hiraoka, Y. F. Liao, K. D. Tsuei, A. Tanaka, L. Hao Tjeng, C. T. Chen, and J. M. Chen, Relation between the Co-O bond lengths and the spin state of Co in layered cobaltates: A high-pressure study, Sci. Rep. **7**, 3656 (2017).

[15] S. Agrestini, C.-Y. Kuo, D. Mikhailova, K. Chen, P. Ohresser, T. W. Pi, H. Guo, A. C. Komarek, A. Tanaka, Z. Hu, and L. H. Tjeng, Intricacies of the Co^{3+} spin state in $Sr_2Co_{0.5}Ir_{0.5}O_4$: An x-ray absoption and magnetic circular dichroism study, Phys. Rev. B **95**, 245131 (2017).

[16] R. H. Potze, G. A. Sawatzky, and M. Abbate, Possibility for an intermediate-spin ground state in the charge-transfer material $SrCoO_3$, Phys. Rev. B **51**, 11501 (1995).

[17] H.-J. Lin, Y. Y. Chin, Z. Hu, G. J. Shu, F. C. Chou, H. Ohta, K. Yoshimura, S. Hebert, A. Maignan, A. Tanaka, L. H. Tjeng, and C. T. Chen, Local orbital occupation and energy levels of Co in Na_xCoO_2: A soft x-ray absorption study, Phys. Rev. B **81**, 115138 (2010).

[18] H. Ohta, K. Yoshimura, Z. Hu, Y. Y. Chin, H. J. Lin, H. H. Hsieh, C. T. Chen, and L. H. Tjeng, Determination of the Co Valence in Bilayer Hydrated Superconducting $Na_xCoO_2.yH_2O$ by Soft x-ray Absorption Spectroscopy, Phys. Rev. Lett. **107**, 066404 (2011).

[19] F. Guillou, Q. Zhang, Z. Hu, C. Y. Kuo, Y. Y. Chin, H. J. Lin, C. T. Chen, A. Tanaka, L. H. Tjeng, and V. Hardy, Coupled valence and spin state transition in $(Pr_{0.7}Sm_{0.3})_{0.7}Ca_{0.3}CoO_3$, Phys. Rev. B **87**, 115114 (2013).

[20] Y. Y. Chin, Z. Hu, H. J. Lin, S. Agrestini, J. Weinen, C. Martin, S. Hébert, A. Maignan, A. Tanaka, J. C. Cezar, N. B. Brookes, Y. F. Liao, K. D. Tsuei, C. T. Chen, D. I. Khomskii, and L. H. Tjeng, Spin-orbit coupling and crystal-field distortions for a low-spin $3d^5$ state in $BaCoO_3$, Phys. Rev. B **100**, 205139 (2019).

[21] A. Podlesnyak, M. Russina, A. Furrer, A. Alfonsov, E. Vavilova, V. Kataev, B. Buchner, T. Strassle, E. Pomjakushina, K. Conder, and D. I. Khomskii, Spin-State Polarons in Lightly-Hole-Doped $LaCoO_3$, Phys. Rev. Lett. **101**, 247603 (2008).

[22] C. He, S. El-Khatib, J. Wu, J. W. Lynn, H. Zheng, J. F. Mitchell, and C. Leighton, Doping fluctuation-driven magneto-electronic phase diagram, in $La_{1-x}Sr_xCoO_3$, Europhys. Lett. **87**, 27006 (2009).

[23] A. Alfonsov, E. Vavilova, V. Kataev, B. Büchner, A. Podlesnyak, M. Russina, A. Furrer, Th. Strässle, E. Pomjakushina, K. Conder, and D. I. Khomskii, Origin of a spin-state polaron in lightly doped $LaCoO_3$, J. Phys.: Conf. Series **150**, 042003 (2009).

[24] V. Kataev, A. Alfonsov, E. Vavilova, A. Podlesnyak, D. I. Khomskii, and B. Büchner, Formation of magnetic polarons in lightly Ca doped $LaCoO_3$, J. Phys.: Conf. Series **200**, 012080 (2010).

[25] A. Podlesnyak, G. Ehlers, M. Frontzek, A. S. Sefat, A. Furrer, T. Strässle, E. Pomjakushina, K. Conder, F. Demmel, and D. I. Khomskii, Effect of carrier doping on the formation and collapse of magnetic polarons in lightly hole-doped $La_{1-x}Sr_xCoO_3$, Phys. Rev. B **83**, 134430 (2011).

[26] Y. Long, Y. Kaneko, S. Ishiwata, Y. Taguchi, and Y. Tokura, Synthesis of cubic $SrCoO_3$ single crystal and its anisotropic magnetic and transport properties, J. Phys.: Condens. Matter **23**, 245601 (2011).

[27] E. Pellegrin, N. Nücker, J. Fink, S. L. Molodtsov, A. Gutiérrez, E. Navas, O. Strebel, Z. Hu, M. Domke, G. Kaindl, S. Uchida, Y. Nakamura, J. Markl, M. Klauda, G. Saemann-Ischenko, A. Krol, J. L. Peng, Z. Y. Li, and R. L. Greene, Orbital character of states at the Fermi level in $La_{2-x}Sr_xCuO_4$ and $R_{2-x}Ce_xCuO_4$ (R = Nd, Sm), Phys. Rev. B **47**, 3354 (1993).

[28] Z. Hu, S. L. Drechsler, J. Málek, H. Rosner, R. Neudert, M. Knupfer, M. S. Golden, J. Fink, J. Karpinski, G. Kaindl, C. Hellwig, and Ch. Jung, Doped holes in edge-shared CuO_2 chains and the dynamic spectral weight transfer in X-ray absorption spectroscopy, Europhys. Lett. **59**, 135 (2002).

[29] L. H. Tjeng, C. T. Chen, and S. W. Cheong, Comparative soft-x-ray resonant-photoemission study on $Bi_2Sr_2CaCu_2O_8$, CuO, and Cu_2O, Phys. Rev. B **45**, 8205 (1992).

[30] T. Burnus, Z. Hu, H. H. Hsieh, V. L. J. Joly, P. A. Joy, M. W. Haverkort, H. Wu, A. Tanaka, H.-J. Lin, C. T. Chen, and L. H. Tjeng, Local electronic structure and magnetic properties of $LaMn_{0.5}Co_{0.5}O_3$ studied by x-ray absorption and magnetic circular dichroism spectroscopy, Phys. Rev. B **77**, 125124 (2008).

[31] S. Agrestini, C.-Y. Kuo, K. Chen, Y. Utsumi, D. Mikhailova, A. Rogalev, F. Wilhelm, T. Förster, A. Matsumoto, T. Takayama, H. Takagi, M. W. Haverkort, Z. Hu, and L. H. Tjeng, Probing the $J_{\text{eff}} = 0$ ground state and the Van Vleck paramagnetism of the Ir^{5+} ions in layered $Sr_2Co_{0.5}Ir_{0.5}O_4$, Phys. Rev. B **97**, 214436 (2018).

[32] W. T. Chen, M. Mizumaki, H. Seki, M. S. Senn, T. Saito, D. Kan, J. P. Attfield, and Y. Shimakawa, A half-metallic A- and B-site-ordered quadruple perovskite oxide $CaCu_3Fe_2Re_2O_{12}$ with large magnetization and a high transition temperature, Nat. Commun. **5**, 3909 (2014).

[33] H. Deng, M. Liu, J. Dai, Z. Hu, C. Kuo, Y. Yin, J. Yang, X. Wang, Q. Zhao, Y. Xu, Z. Fu, J. Cai, H. Guo, K. Jin, T. Pi, Y. Soo, G. Zhou, J. Cheng, K. Chen, P. Ohresser, Y.-f. Yang, C. Jin, L.-H. Tjeng, and Y. Long, Strong enhancement of spin ordering by A-site magnetic ions in the ferrimagnet $CaCu_3Fe_2Os_2O_{12}$, Phys. Rev. B **94**, 024414 (2016).

[34] G. van der Laan and B. T. Thole, Local Probe for Spin-Orbit Interaction, Phys. Rev. Lett. **60**, 1977 (1988).

[35] B. T. Thole and G. van der Laan, Branching ratio in x-ray absorption spectroscopy, Phys. Rev. B **38**, 3158 (1988).

[36] A. Tanaka and T. Jo, Resonant $3d$, $3p$, and $3s$ photoemission in transition metal oxides predicted at $2p$ threshold, J. Phys. Soc. Jpn. **63**, 2788 (1994).

[37] F. M. F. de Groot, X-ray absorption and dichroism of transition metals and their compounds, J. Electron Spectrosc. Relat. Phenom. **67**, 529 (1994).

[38] Parameters for the $Co^{4+}O_6$ cluster calculations: Coulomb energies $U_{3d3d} = 5.0$ eV and $U_{3d2p} = 6.0$ eV; $V_{\text{eg}} = 2.3$ eV. The Slater integrals are reduced to 70% of the Hartree-Fock atomic values for the $3d^5$, $3d^6\underline{L}$, $3d^7\underline{L}^2$, and $3d^8\underline{L}^3$ configurations in the initial state and the $3d^6\underline{p}$, $3d^7\underline{p}\underline{L}$, $3d^8\underline{p}\underline{L}^2$, and $3d^9\underline{p}\underline{L}^3$ configurations in the final state of Co-$L_{2,3}$ XAS, where $\underline{p}$ denotes the Co $2p$ core hole. $10\,\text{Dq} = 0.6$ eV and $T_{\text{pp}} = 0.5$ eV. O 2p to Co 3d charge transfer energy $\Delta = -4.5$ eV, -3.6 eV, and -3.2 eV for the LS, IS, and HS, respectively.

[39] J. Ghijsen, L. H. Tjeng, J. van Elp, H. Eskes, J. Westerink, G. A. Sawatzky, and M. T. Czyzyk, Electronic structure of Cu_2O and CuO, Phys. Rev. B **38**, 11322 (1988).

[40] J. van Elp and A. Tanaka, Threshold electronic structure at the oxygen K edge of $3d$-transition-metal oxides: A configuration interaction approach, Phys. Rev. B **60**, 5331 (1999).

[41] T. Mizokawa, H. Namatame, A. Fujimori, K. Akeyama, H. Kondoh, H. Kuroda, and N. Kosugi, Origin of the Band Gap in the Negative Charge-Transfer-Energy Compound $NaCuO_2$, Phys. Rev. Lett. **67**, 1638 (1991).

[42] T. Mizokawa, A. Fujimori, H. Namatame, K. Akeyama, and N. Kosugi, Electronic structure of the local-singlet insulator $NaCuO_2$, Phys. Rev. B **49**, 7193 (1994).

[43] P. G. Radaelli and S. W. Cheong, Structural phenomena associated with the spin-state transition in $LaCoO_3$, Phys. Rev. B **66**, 094408 (2002).

[44] I. Yamada, T. Odake, A. Tanaka, Y. Okazaki, F. Toda, Y. Ishii, T. Taniguchi, S. Kawaguchi, and A. Hariki, A sequential electron doping for quadruple perovskite oxides $ACu_3Co_4O_{12}$ (A = Ca, Y, Ce), Inorg. Chem. **59**, 8699 (2020).

[45] Q. Huang, J. W. Lynn, B. H. Toby, M. L. Foo, and R. J. Cava, Characterization of the structural transition in $Na_{0.75}CoO_2$, J. Phys.: Condens. Matter **17**, 1831 (2005).

[46] A. Maignan, V. Caignaert, B. Raveau, D. Khomskii, and G. A. Sawatzky, Thermoelectric Power of $HoBaCo_2O_{5.5}$: Possible Evidence of the Spin Blockade in Cobaltites, Phys. Rev. Lett. **93**, 026401 (2004).

[47] C. F. Chang, Z. Hu, H. Wu, T. Burnus, N. Hollmann, M. Benomar, T. Lorenz, A. Tanaka, H. J. Lin, H. H. Hsieh, C. T. Chen, and L. H. Tjeng, Spin Blockade, Orbital Occupation, and Charge Ordering in $La_{1.5}Sr_{0.5}CoO_4$, Phys. Rev. Lett. **102**, 116401 (2009).